Electronic Supplementary information (ESI)

For

Tuning the light absorption of a molecular vanadium oxide system for enhanced photooxidation performance

Johannes Forster, Benedikt Rösner, Marat M. Khusniyarov and Carsten Streb*

Department Chemistry and Pharmacy, Institute of Inorganic Chemistry II, Friedrich-Alexander-University Erlangen-Nuremberg, Egerlandstr. 1, 91058 Erlangen, Germany.
*Email: carsten.streb@chemie.uni-erlangen.de

1. Instrumentation

X-ray diffraction: Single-crystal X-ray diffraction studies were performed on a Nonius Kappa CCD Single-crystal X-ray diffractometer equipped with a graphite monochromator using MoKα radiation (wavelength λ(Mo-k_α) = 0.71073Å).

NMR spectroscopy: ^{1}H- and ^{13}C-NMR spectroscopy were performed on a JEOL EX 270 NMR spectrometer or JEOL EX 400 spectrometer using deuterated solvents as internal standards.

UV-Vis spectroscopy: UV-Vis spectroscopy was performed on a Shimadzu UV-2401PC spectrophotometer, Varian Cary 50 spectrophotometer or Varian Cary 5G spectrophotometer equipped with a Peltier thermostat. All systems were used with standard cuvettes (d = 10.0 mm) or with specialized Hellma UV-Vis flow cells connected to a Heidolph PD5201 peristaltic pump.

Gas chromatography: Analysis of the organic reaction products was performed on a Shimadzu GC 17A gas chromatograph equipped with a thermal conductivity detector (TCD) system. Methanol, formaldehyde and formic acid were used as reference samples.

FT-IR spectroscopy: FT-IR spectroscopy was performed on a Shimadzu FT-IR-8400S spectrometer. Samples were prepared as KBR pellets. Signals are given as wavenumbers in cm^{-1} using the following abbreviations: vs = very strong, s = strong, m = medium, w = weak and b = broad.

Elemental analysis: Elemental analysis was performed on a Euro Vector Euro EA 3000 Elemental Analyzer.

General remarks: All chemicals were purchased from Sigma Aldrich or ACROS and were of reagent grade. The chemicals were used without further purification unless stated otherwise.

2. Synthetic section:

2.1. Synthesis of **{V_4}**: $((n\text{-}C_4H_9)_4N)_4[V_4O_{12}]$:

The synthesis of $((n\text{-}C_4H_9)_4N)_4[V_4O_{12}]$ is a modified version of a published procedure:[S1] V_2O_5 (10.0 g, 55.0 mmol) is suspended in deionized water (30 ml). To this, an aqueous solution of $(n\text{-}C_4H_9)_4NOH$ (72 ml, 1.53 M) is added together with H_2O (10 ml). The reaction was vigorously stirred and heated to 80 ° C overnight. A clear, almost colourless solution was obtained which was evacuated to dryness using a rotavap, giving an off-white solid. Yield: 35.7 g (26.2 mmol, 95.1 % based on V).
Elemental analysis for $C_{64}H_{144}N_4V_4O_{12}$ in wt.-% (calcd.): C 56.13 (56.23), H 10.77 (10.63), N 4.04 (4.10).
Characteristic IR bands (in cm^{-1}): 3428 (b), 2945 (s), 2362 (w), 1618 (m), 1473 (vs), 1379 (m), 1283 (w), 1167 (m), 1109 (m), 1031 (m), 964 (s), 908 (s), 850 (m), 736 (m), 696 (s).
Characteristic UV-Vis signals (in acetonitrile): λ_{max} = 285 nm, ε= 1.12 x 10^4 M^{-1} cm^{-1}.

2.2. Synthesis of **{V_5}**: $((n\text{-}C_4H_9)_4N)_3[V_5O_{14}]$:

This compound is identical to the material reported previously by Day, Klemperer and Yaghi.[S2] However, the synthetic procedure is different to the original synthesis.
A sample of $((n\text{-}C_4H_9)_4N)_4[V_4O_{12}]$ (1.0 g, 0.73 mmol) was dissolved in acetonitrile or DMF (10 ml) and heated to 80 ° C for 2 h. The hot solution was filtered and poured into 100 ml diethyl ether. A yellow oily precipitate was centrifuged off and vacuum-dried on a vacuum line. A yellow solid was obtained. Yield: 766 mg (0.64 mmol, 87.7 % of crude product based on V).
Elemental analysis for $C_{48}H_{108}N_3O_{14}V_5$ x 0.65 $C_{16}H_{37}NO$ in wt.-% (calcd.) C 51.02 (51.02), H 10.35 (9.68), N 3.70 (3.72).
Characteristic IR bands (in cm^{-1}): 3430 (b), 2920 (s), 2874 (m), 1632 (m), 1474 (vs), 1166 (m), 1109 (m), 922 (vs), 850 (m), 736 (s), 676 (s), 581 (w), 500 (w).
Characteristic UV-Vis signals (in acetonitrile): λ_{max} = 360 nm, ε= 0.93 x 10^4 M^{-1} cm^{-1}.
The presence of the $[V_5O_{14}]^{3-}$ cluster was also verified using single-crystal X-ray diffraction studies, see section 3.

2.3. Synthesis of **{V_{10}}**: $((n\text{-}C_4H_9)_4N)_4[V_{10}O_{26}]$ x 2 DMF:

$((n\text{-}C_4H_9)_4N)_4[V_4O_{12}]$ (1.0 g, 0.73 mmol) was dissolved in DMF (25 ml) and N-*tert*-butyl diethanolamine (5 eq., 611 mg, 3.8 mmol) (or 5 equivalents of another alcohol, e.g. MeOH, EtOH, etc.) was added. The reaction was heated to 90 ° C and exposed to sunlight or irradiated with a 50 W halogen tungsten light source over night. The colour gradually changed to deep purple. After cooling to room temperature, the solution was centrifuged. Diffusion of diethyl ether into the reaction mixture gave purple needle crystals. Yield: 304 mg (0.182 mmol, 62.5 % based on V). The reaction can also be carried out in acetonitrile or DMSO under otherwise unchanged reaction conditions, giving similar yields.
Elemental analysis for a dried sample of compound **{V_{10}}**, sum formula $C_{64}H_{144}N_4V_{10}O_{26}$ in wt.-% (calcd.): C 40.96 (40.56), H 7.67 (7.66), N 3.07 (2.96).
Characteristic IR bands (in cm^{-1}): 3435 (b), 2961 (vs), 2874 (s), 1668 (s), 1636 (m), 1485 (s), 1464 (m), 1382 (s), 1153 (w), 970 (s), 842 (vs), 530 (w).
Characteristic UV-Vis signals (in acetonitrile): λ_{max} = 500 nm, ε= 1.73 x 10^3 M^{-1} cm^{-1}.

2.4. Crystallization of **{V_5}**: $((n\text{-}C_4H_9)_4N)_7[V_5O_{14}]_1[V_{10}O_{26}]_1$ x n DMF

Aim of the synthesis of this compound was the crystallization of the $[V_5O_{14}]^{3-}$ cluster **{V_5}**. The proposed light-induced **{V_{10}}** formation requires the co-existence of the $[V_5O_{14}]^{3-}$ unit and the $[V_{10}O_{26}]^{4-}$ unit (i.e. in principle the reduced and oxidized vanadate cluster species can be present in solution at the same time without any interfering redox-reactions occurring). To prove the co-existence of these two clusters and to demonstrate the presence of the **{V_5}** species during the photocatalysis as a well-defined unit, we conducted the standard light-induced **{V_{10}}** formation setup (see 2.5) but interrupted the reaction approximately halfway through, before all the **{V_5}** units were reduced to the **{V_{10}}** species. Fast crystallization of the reaction mixture by diffusion of diethyl ether into the mother liquor to avoid rearrangement of the **{V_5}** units back to the **{V_4}** precursor gave $((n\text{-}C_4H_9)_4N)_7[V_5O_{14}]_1[V_{10}O_{26}]_1$ x n DMF as purple needle crystals in variable yields of ca. 10-15 % based on V. This compound consists of one 2-electron reduced {**V_{10}**} cluster and one fully oxidized **{V_5}** cluster and verifies the possibility of both clusters being present in the same reaction mixture.

2.5. Light-induced **{V_{10}}** formation reaction and UV-Vis monitoring

In a typical photochemical **{V_{10}}** formation reaction, $((n\text{-}C_4H_9)_4N)_4[V_4O_{12}]$ (250 mg, 0.18 mmol) was dissolved in 100 ml of the solvent (acetonitrile, DMF, DMSO) together with 5-20 equivalents of the corresponding alcohol. The reaction mixture was heated to the desired temperature (50 – 90 ˚ C) and the reaction was irradiated using a standard 50 W tungsten halogen light source (Osram HALOPAR 50 W) equipped with a UV cutoff filter (cutoff wavelength 380 nm) and the reaction mixture was pumped through the UV-Vis flow cell with a flow rate of ca. 5 ml min^{-1}. Data points were collected at a rate of 1 min^{-1}.

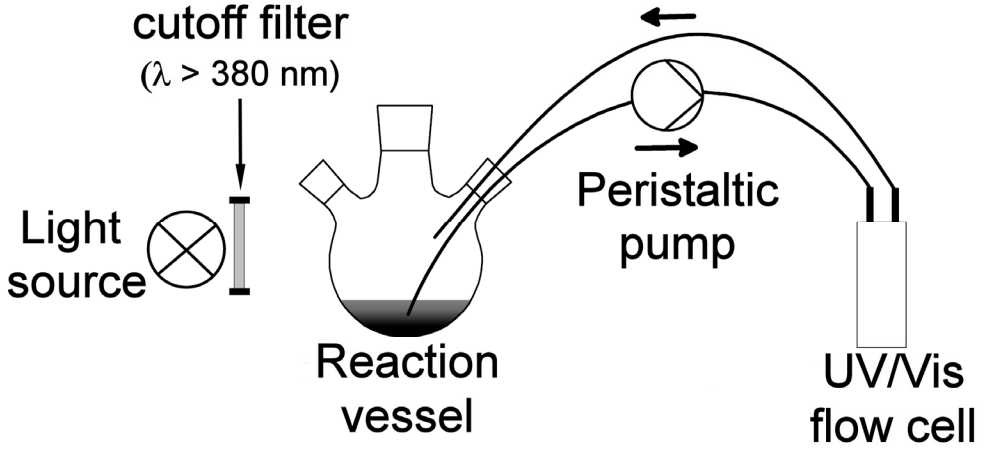

Figure S 1: Illustration of the experimental monitoring of the photocatalytic reaction. Visible light from a standard 50 W tungsten halogen light source (Osram HALOPAR 50 W) equipped with a UV cutoff filter (380 nm, Green.L dHD) was used to irradiate a standard reaction flask. The reaction mixture was continuously pumped (Heidolph PD5201 peristaltic pump) through a flowcell (HELLMA QC grade 89 ul). UV-spectrometric measurements were performed using a Shimadzu UV-2401PC UV-Vis spectrometer or a Varian Cary 50 UV-Vis spectrometer.

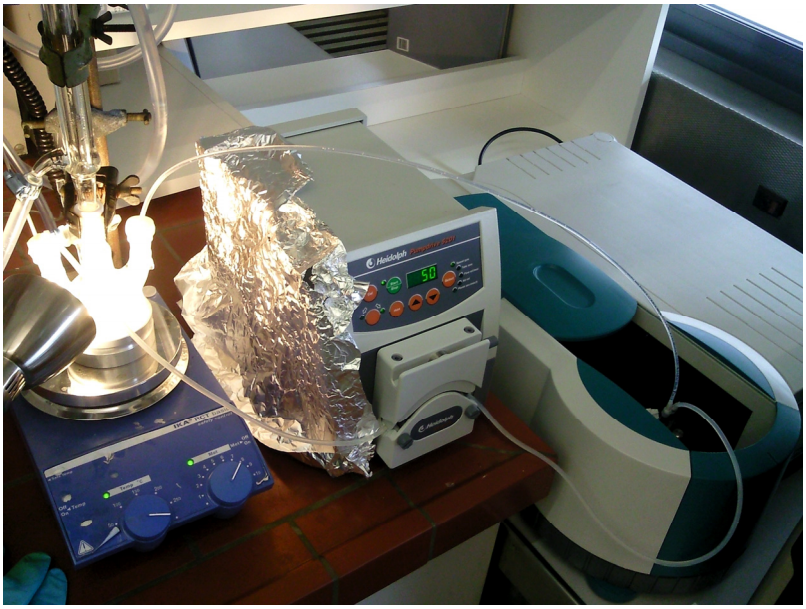

Figure S 2: Photograph of the flow cell UV-Vis spectroscopic setup

3. Crystallographic information

Single-Crystal Structure Determination: Suitable single crystals of the respective compound were grown and mounted onto the end of a thin glass fiber using Fomblin oil. X-ray diffraction intensity data were measured at 150 K on a Nonius Kappa CCD diffractometer [λ(Mo-K_α) = 0.71073 Å] equipped with a graphite monochromator. Structure solution and refinement was carried out using the SHELX-97 package[S3] *via* WinGX.[S4] Corrections for incident and diffracted beam absorption effects were applied using empirical[S5] or numerical methods.[S6] Structures were solved by a combination of direct methods and difference Fourier syntheses and refined against F^2 by the full-matrix least-squares technique. Crystal data, data collection parameters and refinement statistics are listed in Table S1. These data can be obtained free of charge via www.ccdc.cam.ac.uk/conts/retrieving.html or from the Cambridge Crystallographic Data Center, 12, Union Road, Cambridge CB2 1EZ; fax:(+44) 1223-336-033; or deposit@ccdc.cam.ac.uk. CCDC reference numbers 794192 (**{V_{10}}**) and 794193 (**{V_5}{V_{10}}**).

Table S1: Summary of the crystallographic information

	$((n\text{-}C_4H_9)_4N)_4[V_{10}O_{26}]$ x 2DMF	$((n\text{-}C_4H_9)_4N)_4[V_5O_{14}][V_{10}O_{26}]$ x n DMF
Formula	$C_{70}H_{158}N_6O_{28}V_{10}$	$C_{112}H_{252}N_7O_{40}V_{15}$
M_r g mol^{-1}	2041.42	3101.34
crystal system	Orthorhombic	Monoclinic
space group	$P2_12_12_1$	$P2_1/n$
a [Å]	16.9781(2)	18.4325(17)
b [Å]	17.7089(3)	17.0098(17)
c [Å]	32.9662(4)	49.5090(30)
α [°]	90	90
β [°]	90	97.192(7)
γ [°]	90	90
ρ_{cald} [g cm^{-3}]	1.368	1.337
V [Å^3]	9911.7(2)	15400.6(1)
Z	4	4
$\mu(Mo_{K\alpha})$ mm^{-1}	0.966	0.928
T [K]	150(2)	150(2)
no. rflns (measd)	70625	200957
no. rflns (unique)	20202	28096
no. params	1021	1432
*R*1 (I>2σ(I)	0.0432	0.0692
*wR*2 (all data)	0.1087	0.2069
GooF	1.049	1.008

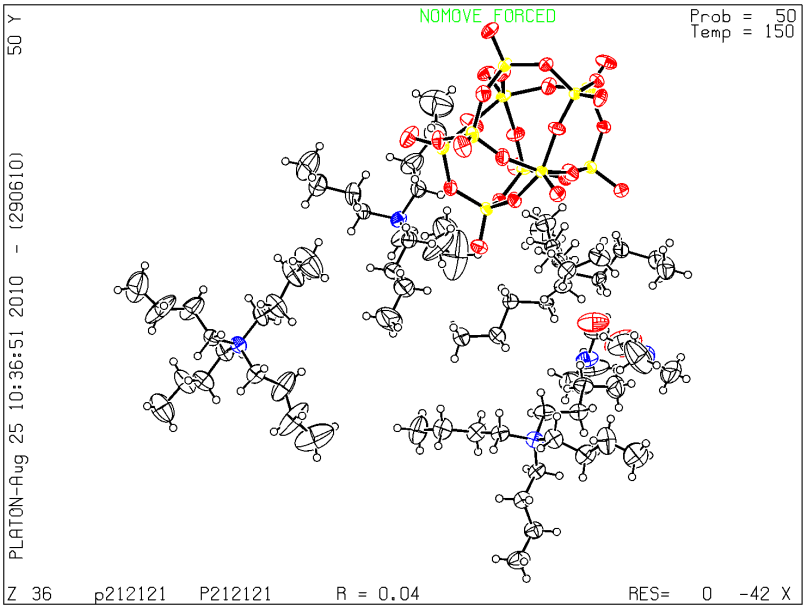

Figure S 3: ORTEP-plot of $((n\text{-}C_4H_9)_4N)_4[V_{10}O_{26}]$ x 2 DMF, probability ellipsoids given at 50 %. The anisotropic parameters of the C-atoms in the $(n\text{-}C_4H_9)_4N^+$ tetra-*n*-butylammonium cations are slightly enlarged due to structural disorder within the structure. Despite this disorder, the structure was refined fully anisotropically to satisfactory R values.

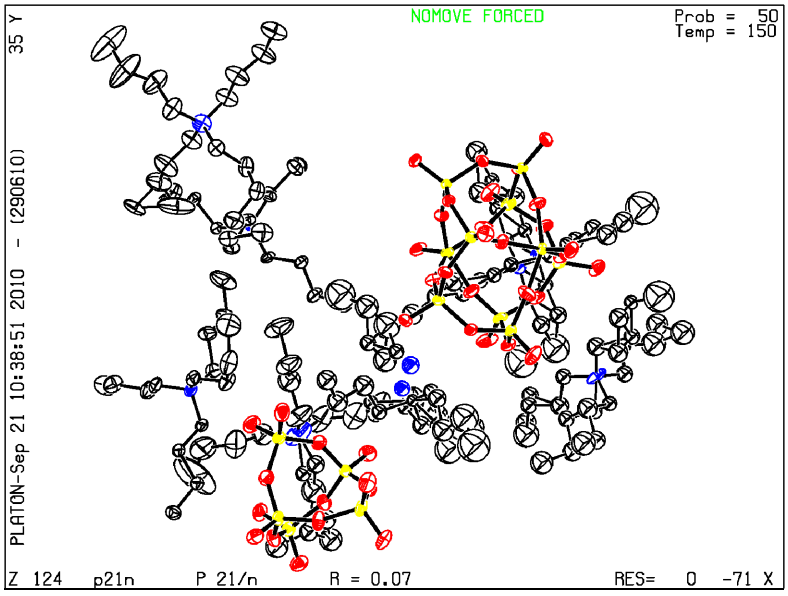

Figure S 4: ORTEP-plot of $((n\text{-}C_4H_9)_4N)_4[V_5O_{14}][V_{10}O_{26}]$ x n DMF, probability ellipsoids given at 50 %. The atoms of the two $(n\text{-}C_4H_9)_4N^+$ tetra-*n*-butylammonium cations based around N1/N1A and N2/N2A were refined isotropically due to strong structural disorder. The two vanadium oxide clusters and the five remaining tetra-*n*-butylammonium cations (N3 – N7-based) were refined fully anisotropically. This allowed refinement of the structure to satisfactory R values.

Characterization of the oxidation state of the vanadate clusters using bond valence sum calculations

Compound 3:
$[V_{10}O_{26}]^{4-}$ cluster in compound 3

Atom Name	Bond valence sum parameter	Atom Name	Bond valence sum parameter
V1	4.393	V6	5.202
V2	5.180	V7	5.216
V3	5.212	V8	5.225
V4	4.484	V9	5.241
V5	5.166	V10	5.179

This calculation indicates that the vanadium centers V1 and V4 are in oxidation state +IV whereas the remaining vanadium centers are in oxidation state +V. This is in line with the structural analysis as the vanadium centers V1 and V4 occupy the apical positions and the remaining eight vanadium centers form the central belt.

Compound 4:
$[V_{10}O_{26}]^{4-}$ cluster in compound **4**

Atom Name	Bond valence sum parameter	Atom Name	Bond valence sum parameter
V1	4.376	V6	5.115
V2	5.080	V7	5.046
V3	5.111	V8	5.191
V4	4.387	V9	5.099
V5	5.038	V10	5.115

This calculation indicates that the vanadium centers V1 and V4 are in oxidation state +IV whereas the remaining vanadium centers are in oxidation state +V. This is in line with the structural analysis as the vanadium centers V1 and V4 occupy the apical positions and the remaining eight vanadium centers form the central belt.

$[V_5O_{14}]^{3-}$ cluster in compound **4**

Atom Name	Bond valence sum parameter
V11	5.187
V12	5.058
V13	5.228
V14	5.127
V15	5.189

This calculation indicates that all vanadium centers of the **{V_5}** cluster are in oxidation state +V. This is in line with the previous structural report of this cluster by Day, Klemperer and Yaghi.[S2]

4. UV-Vis spectroscopic investigations

4.1. UV-Vis spectroscopy of the **{V_5}**-**{V_{10}}** reduction reaction

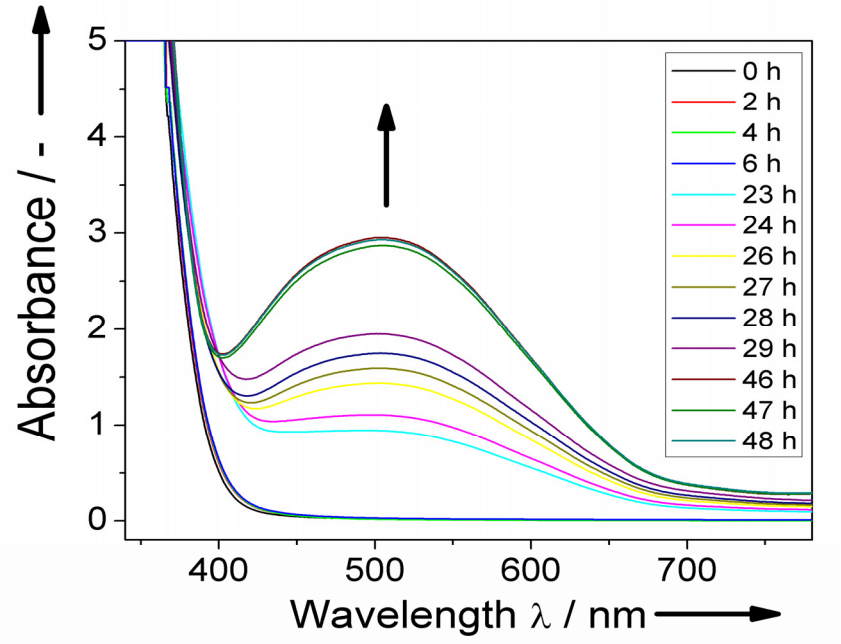

Figure S 5: UV-Vis spectroscopic observation of the formation of the **{V_{10}}** cluster indicated by the appearance of an inter-valence charge-transfer (IVCT) band at λ_{max} = 500 nm.

4.2. UV-Vis spectroscopy of the **{V_{10}}**-**{V_5}** re-oxidation reaction using O_2

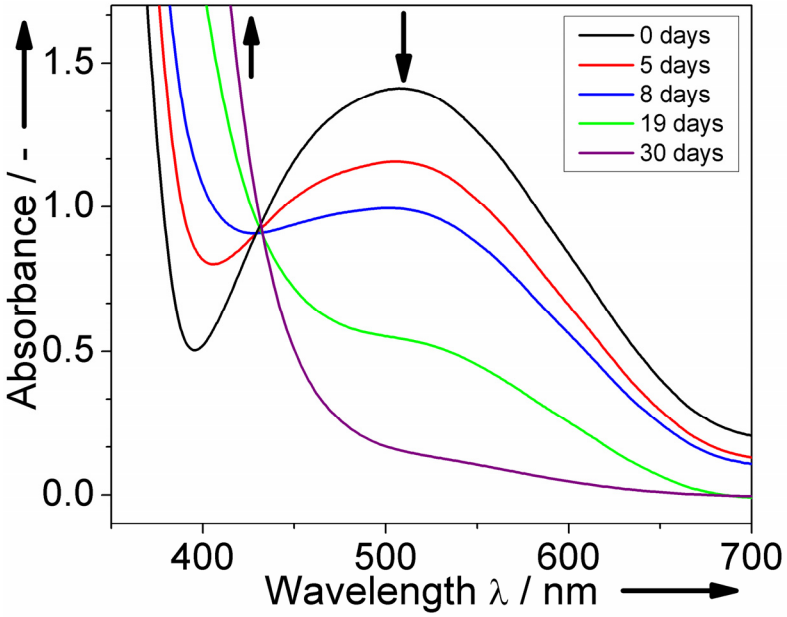

Figure S 6: Re-oxidation of the **{V_{10}}** cluster to the fully oxidized **{V_5}** unit followed by time-dependent UV-Vis measurements. The signal at λ_{max} = 500 nm characteristic of the **{V_{10}}** species disappears over time while the high-intensity LMCT band at λ_{max} = 360 nm (characteristic of **{V_5}**) increases. An isosbestic point is observed at $\lambda_{isosbestic}$ = 431 nm.

4.3 UV-Vis spectroscopy of the **{V_{10}}-{V_5}** re-oxidation reaction using H_2O_2

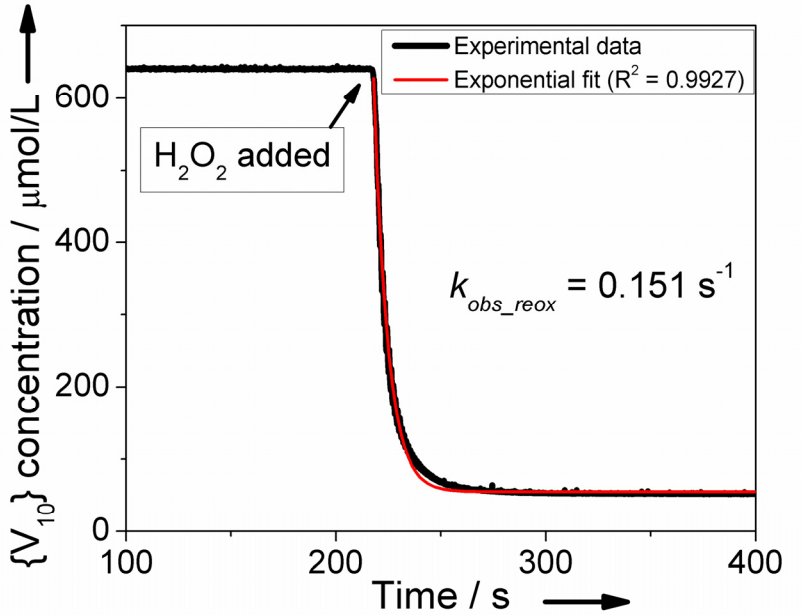

Figure S 7: UV-Vis spectroscopic monitoring of the redox cycling of the **{V_5}-{V_{10}}** system. A standard photocatalytic substrate oxidation reaction under optimized conditions is performed to give an observed **{V_{10}}** concentration of ca. 620 μmol/L. As the maximum **{V_{10}}** concentration was achieved, the reaction was allowed to equilibrate and at t = 210 s, a slight excess of aqueous hydrogen peroxide (220 μl, 35 wt.-%) was added. The **{V_{10}}** cluster is almost instantly re-oxidized to the **{V_5}** cluster and the theoretical fit of the observed pseudo first-order reaction rate allowed us to calculate the observed rate constant k_{obs_reox} = 0.151 s^{-1}. Experimental conditions: Solvent: DMSO/H_2O (9:1, v:v), T = 70 ° C, data collection at a rate of 10 data points per second.

5. Identification of the organic oxidation products

In order to analytically identify the organic oxidation products, a series of photocatalytic test reactions were conducted using methanol as a prototype primary alcohol. The reaction series were carried out under visible light irradiation on a standard scale and in deuterated solvents for NMR-studies; the reaction products were analyzed using ^{1}H-NMR spectroscopy and GC-TCD (thermal conductivity detector) analysis.

Both ^{1}H-NMR spectroscopy and GC-TCD analysis using formaldehyde and formic acid as external references showed that methanol was selectively oxidized to the corresponding formaldehyde and no formic acid was observed spectroscopically or by gas chromatography, see below. In addition to the observation of the formaldehyde, the ^{1}H-NMR study of the reaction indicates the appearance of a water signal which is in line with the proposed reaction mechanism for the methanol oxidation and {V_{10}} generation, see below:

Proposed formal reaction mechanism:

Reduction: $2\,[V_5O_{14}]^{3-} + 2\,e^- \rightarrow [V_{10}O_{26}]^{4-} + 2\,O^{2-}$
Oxidation: $CH_3OH \rightarrow H_2CO + 2\,e^- + 2\,H^+$

Net reaction: $2\,[V_5O_{14}]^{3-} + CH_3OH \rightarrow [V_{10}O_{26}]^{4-} + H_2CO + 2\,OH^-$
Water formation: $CH_3OH + OH^- \rightarrow CH_3O^- + H_2O$ (equilibrium is on the left)

5.1. Gas chromatographic (GC-TCD) product analysis

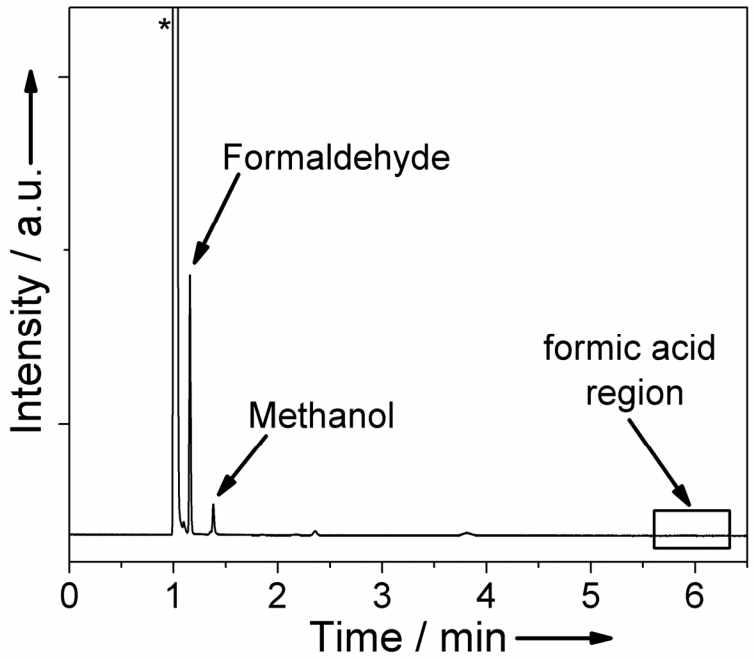

Figure S8: Gas chromatographic analysis of the reaction products formed during the visible-light induced $\{V_{10}\}$ formation and methanol oxidation. Only the reagent methanol(t = 1.38 min) and the primary oxidation product formaldehyde (t = 1.14 min) are observed chromatographically. No signal was observed in the expected formic acid region centered on t = 5.92 min. The expected elution times were determined using methanol, formaldehyde and formic acid as external references. The solvent signal (DMSO) is marked with an asterisk.

5.2. ^{1}H-NMR spectroscopic analysis

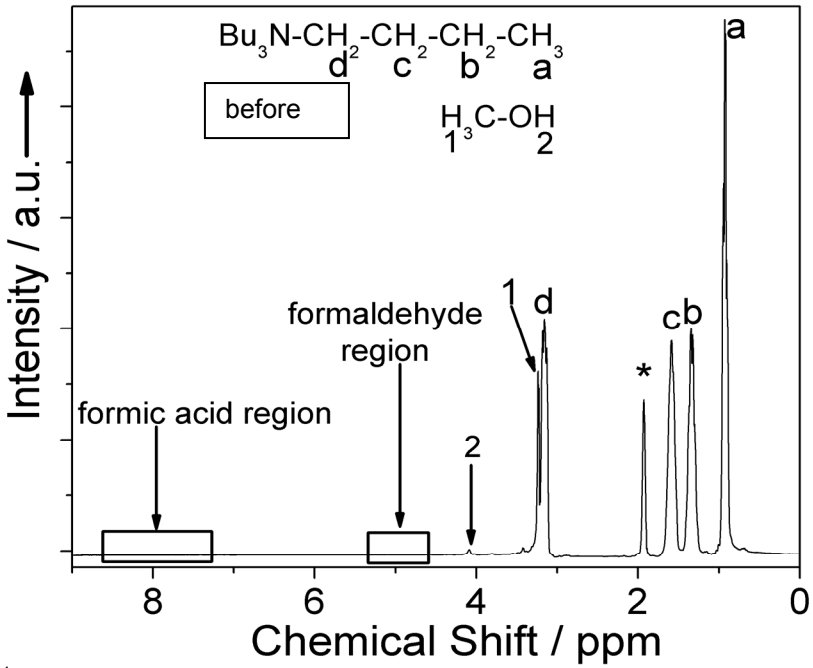

Figure S 9: ^{1}H-NMR spectrum of the reaction mixture before exposure to visible light. Only the expected signals for the tetra-*n*-butylammonium counter ion, for methanol and for the solvent (acetonitrile-d3) are observed. No signals are observed for formaldehyde or formic acid. Solvent signal marked with an asterisk.

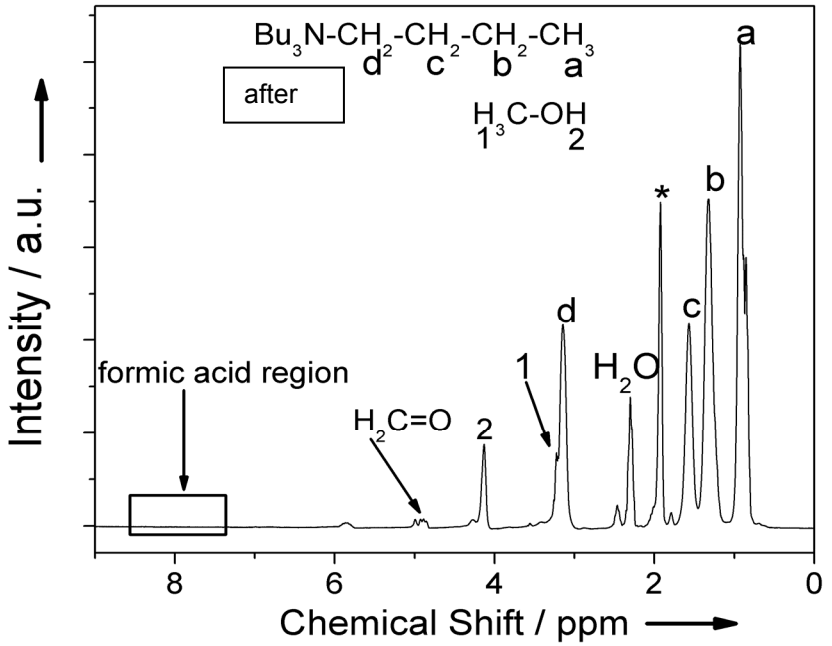

Figure S 10: ^{1}H-NMR spectrum of the reaction mixture after exposure to visible light for 24 h. After the light-induced reaction, a signal for formaldehyde can be observed at δ = 4.90 ppm. This is in line with the external reference sample for formaldehyde collected under identical conditions. No signal was observed for formic acid which is expected at δ = 8.0 ppm based on reference samples measured under identical conditions. In addition,

a new signal for water was observed at δ = 2.30. This water formation further indication of the postulated reaction mechanism, see above. In addition, an increased signal for the hydroxyl proton of the methanol was observed, due to D/H exchange with the formed water (signal no. 2, δ = 4.1 ppm). The general line broadening of the spectrum after light exposure is due to the formation of the paramagnetic **{V_{10}}** species and is partly responsible for the modest spectral resolution. The solvent signal (acetonitrile-d3 is marked with an asterisk *, δ = 1.95 ppm).

Additional experiments using 2-propanol as a prototype secondary alcohol indicated that under the standard photooxidative reaction conditions described above (section 2.5), 2-propanol is selectively oxidized to the corresponding ketone, acetone.

6. DFT calculations

The program package ORCA 2.7 revision 0 was used for all calculations.[S7] The calculations were performed on not-optimized structures as obtained from single crystal X-ray diffractometry. The single point calculations were performed with the B3LYP functional.[S8-S9] The triple-ζ basis sets with one set of polarization functions[S10] (TZVP) were used for all atoms. TD-DFT calculations were performed using the B3LYP functional and the conductor like screening model (COSMO)[S11] with acetonitrile as a solvent. The first 100 excited states were calculated, where the maximum dimension of the expansion space in the Davidson procedure (MAXDIM) was set to 1000.

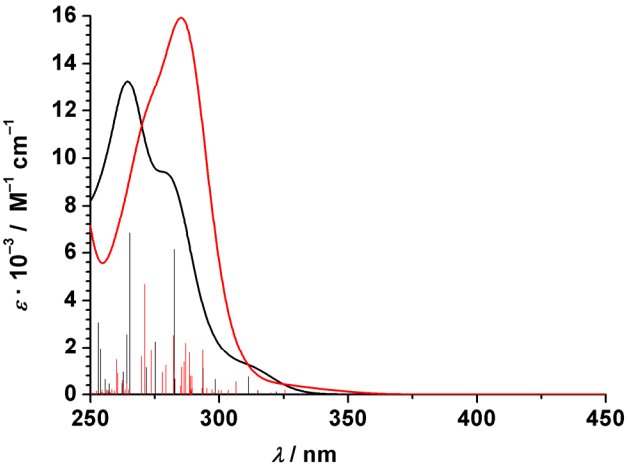

Figure S11. Electronic absorption spectra of **{V_4}** (black) and **{V_5}** (red) as obtained from the spin-restricted B3LYP-TD-DFT calculations including the conductor like screening model (COSMO). The first 100 excited states have been calculated. Full-width at half-maximum (FWHM) height was set to 2000 cm^{-1} for each transition. The HOMO-LUMO gap is decreased by 0.29 eV in going from **{V_4}** to **{V_5}**.

7. Literature references cited in Supporting Information

S1 P. Roman, A. S. Jose, A. Luque, J. M. Gutierrez-Zorrilla, *Inorg. Chem.* 1993, **32**, 775.
S2 V. W. Day, W. G. Klemperer, O. M. Yaghi, *J. Am. Chem. Soc.* 1989, **111**, 4518.
S3 G. M. Sheldrick, *Acta Crystallogr.* 2008, **A64**, 112.
S4 L. J. Farrugia, *J. Appl. Cryst.* 1999, **32**, 837.
S5 R. H. Blessing, *Acta Crystallogr. A* 1995, **51**, 33.
S6 P. Coppens, L. Leiserowitz, D. Rabinovich, *Acta Crystallogr.* 1965, **18**, 1035.
S7 F. Neese, ORCA – an Ab Initio, Density Functional and Semiempirical SCF-MO Package, version 2.7 revision 0; Institut für Physikalische und Theoretische Chemie, Universität Bonn, Germany, 2009.
S8 A. D. Becke, *J. Chem. Phys.*, 1993, **98**, 5648.
S9 C. T. Lee, W. T. Yang and R. G. Parr, *Phys. Rev. B*, 1988, **37**, 785.
S10 A. Schafer, H. Horn and R. Ahlrichs, *J. Chem. Phys.*, 1992, **97**, 2571.
S11 A. Klamt and G. Schuurmann, *J. Chem. Soc., Perkin Trans.* 1993, **2**, 799.